Monatshefte für Chemie 123, 63–72 (1992)

Monatshefte für Chemie
Chemical Monthly

Printed in Austria

Thermal Decomposition of Peroxyacetyl Nitrate in the Presence of O_2, NO_2 and NO

Nikolaos Roumelis and **Sotirios Glavas***

Department of Chemistry, University of Patras, GR-26110 Patras, Greece

Summary. The thermal decomposition of pure *PAN* in N_2 as well as in the presence of added O_2, NO_2 and NO was studied at 1 atm pressure. In addition to methyl nitrate, NO_2 was a significant N-product of pure *PAN* in N_2 thermal decomposition. In the presence of sufficiently large amounts of O_2, no methyl nitrate was formed at 333 K, indicating that the homolytic *PAN* decay to methyl nitrate and carbon dioxide is not occurring. In the presence of NO (in contrast to former studies) methyl nitrite was found to be the major organo-nitrogen compound instead of methyl nitrate. The system $PAN-NO-N_2$ allowed the determination of the rate constant $3.1 \cdot 10^{-4} s^{-1}$ at 298 K for reaction (1): $PAN \rightarrow CH_3COO_2 + NO_2$, in agreement with prior studies. Computer simulations based on the free radical mechanism starting with reaction (1) fitted very well the experimental results.

Keywords. PAN; Thermal decomposition; O_2; NO_2; NO.

Die thermische Zersetzung von Peroxyacetylnitrat in Gegenwart von O_2, NO_2 und NO

Zusammenfassung. Die thermische Zersetzung von reinem *PAN* in N_2 und in Gegenwart von zugemischtem O_2, NO_2 und No wurde bei 1 atm Druck untersucht. Zusätzlich zu Methylnitrat war NO_2 ein signifikantes N-Produkt bei der thermischen Zersetzung von reinem *PAN* in N_2. In Gegenwart genügend großer Mengen von O_2 wurde bei 333 K kein Methylnitrat gebildet. Dies zeigt an, daß der homolytische Zerfall von *PAN* zu Methylnitrat und Kohlendioxid nicht eintritt. Im Gegensatz zu früheren Untersuchungen wurde in Gegenwart von NO nicht Methylnitrat, sondern Methylnitrit als wichtigste Organo-Stickstoff-Verbindung gefunden. Im System $PAN-NO-N_2$ wurde die Geschwindigkeitskonstante, in Übereinstimmung mit früheren Untersuchungen, zu $3.1 \cdot 10^{-4} s^{-1}$ bei 298 K für die Reaktion (1): $PAN \rightarrow CH_3COO_2 + NO_2$ bestimmt. Computersimulierung auf Basis des freien Radikal-Mechanismus beginnend mit Reaktion (1) waren mit den experimentellen Resultaten in sehr guter Übereinstimmung.

Introduction

It is now well established that *PAN* is ubiquitous in the atmosphere. It constitutes a significant compound of photochemical smog in the urban areas all over the world, where it may also be used as an index of photochemical air pollution next to ozone. In clean atmospheres *PAN* has been found to be a significant odd nitrogen reservoir [1].

Since the pioneering work of Stephens and coworkers *PAN* is known to decompose thermally with the two major products being methyl nitrate and carbon

dioxide. These products were proposed to be formed by homolytic decomposition of *PAN* via a six-membered cyclic intermediate [2], reaction (23):

$$CH_3COO_2NO_2 \rightarrow CH_3ONO_2 + CO_2. \quad (23)$$

Several years later Cox and Roffey [3] and Hendry and Kenley [4] proposed a free radical mechanism starting with reaction (1):

$$CH_3COO_2NO_2 \rightleftharpoons CH_3COO_2 + NO_2. \quad (1,-1)$$

The work of Bruckmann and Willner a few years later corroborated that the free radical was the exclusive mechanism of *PAN* thermal decomposition [5]. Recently however, Senum and coworkers proposed that parallel to the free radical mechanism the thermal decomposition of *PAN* is effected by a homolytic pathway [6]. In the most recent study of *PAN* by Wangberg et al. [7], the heterogeneous factors that affect the *PAN* thermal destruction were studied. These authors could not differentiate between the free radical only mechanism and the homolytic plus free radical mechanism proposed by Senum et al. [6]. They reported that reaction (1) is not effected heterogeneously.

In addition to the above differences on the mechanism, a number of discrepancies still exist on the identity and quantity of *PAN* thermal decomposition products. Thus NO_2 (which we find to be a significant product of the pure PAN/N_2 decomposition) was not observed at all in many previous studies [6, 7] whereas Bruckmann and Willner [5] reported qualitatively on the NO_2 formation. Furthermore nitromethane [5, 6] and methyl nitrite [8] were also reported to be products of the pure *PAN* decay without convincing mechanistic explanation. Large discrepancies also exist in the literature in the amounts of methyl nitrate formed from the decay of pure *PAN* [5–7]. Similarly the organo-nitrogen decay products of *PAN* in the presence of NO were also not satisfactorily documented in earlier studies [6, 7].

The purpose of the present work was to examine the significance of the homolytic *PAN* destruction as proposed by Senum et al. compared to the free radical mechanism. Because of the uncertainty in the reported reaction products and their quantitative relationships we studied the products formed under a variety of conditions. Thus using ppbv concentrations, so that extrapolations to ambient conditions would be more reliable, we studied the $PAN-N_2$ system as well as the effect of added O_2, NO_2 and NO on the rate of *PAN* decomposition and we obtained quantitative relationships of the products formed.

Experimental Part

All experiments were carried out at 1 atm pressure using N_2 as matrix, in a 4.5 l glass flask, equipped with two septa ports and a teflon stopcock and thermostated in an oil bath at 50 ± 0.1°C. This vessel was connected to a vacuum line provided with teflon stopcocks. The experiments with NO were carried out in a 425 l glass chamber, thermostated at 23.5 ± 0.5°C.

PAN was prepared starting with the anhydride of acetic acid via peracetic acid [9] which in turn was nitrated to *PAN* according to the procedure of Gaffney et al. [10]. *PAN* was stored in different small vials at −10°C and only one portion was removed from each vial when needed after thawing, in order to avoid its decomposition. Freshly prepared *PAN* was always used and thus the peak of methyl nitrate in the *PAN* introduced in the reaction vessels was negligible. Methyl nitrate [11] and methyl nitrite [12] were synthesized by modification of standard methods. The NO used, of purity

99.8%, was obtained from Messer Griesheim and was used as such. NO_2 was prepared daily in darkened glass flasks from NO and a 9 : 1 excess of high purity O_2. The pressure measurements were made using MKS Baratron capacitance manometers.

PAN, CH_3ONO_2 and CH_3ONO analyses were carried out by injecting 0.5 ml samples using gas tight syringes provided with teflon plungers, into a Hewlett-Packard 5890 A gas chromatograph equipped with a ^{63}Ni electron capture detector and in a Shimadzu Series 8 GC also equipped with a ^{63}Ni electron capture detector. For the separation of *PAN* and CH_3ONO_2 a HP-1, 5-m-long fused silica cross-linked methyl silicone gum column was used, 0.53 mm i.d., 2.65 μm film thickness [13]. When better resolution of methyl nitrate from the air peak was desired a HP-17 column was used, 10-m-long fused silica cross-linked methyl-phenyl silicone, 0.53 mm i.d., 2.65 μm film thickness. Under our operating conditions *PAN* eluted in 2.55 and 3.10 min and methyl nitrate in 0.85 and 1.10 min in the HP-1 and in the HP-17 columns, respectively. Helium was the carrier gas and 10% CH_4/Ar the make-up gas. Methyl nitrite was separated on a 45 cm long glass column, 2 mm i.d. filled with Porapak Q (80/100 Mesh). The use of the Porapak Q column was necessary because the methyl nitrite was not well resolved from the air peak (seen on the ECD) with the HP-1 wide bore column. On the Porapak Q column methyl nitrite was the only eluting compound at 3.25 min. The ovens in both chromatographs were set at 30°C and the HP ECD was operated at 45°C, whereas the Shimadzu ECD was operated at 30°C. The calibration of the ECD's for *PAN*, methyl nitrate and methyl nitrite was carried out using a Pye Unicam GC equipped with a home built NO_x chemiluminescence detector, after their conversion to NO on a Mo-converter operated at 320°C. The NO_x detector could easily be calibrated with standard NO. In addition for the analyses of *PAN*, the ECD's were also calibrated against an ion chromatograph after hydrolysis of *PAN* in an alkaline solution and determination of NO_2^--formed.

NO was determined by its chemiluminescence reaction with ozone. This home built detector was operated at flows 30 ml/min and had a detection limit of 3 ppbv. Unfortunately *PAN*, methyl nitrate, and methyl nitrite were all converted on the Mo-converter to NO with 100% efficiency and therefore they contributed 100% to the signal in the NO_2 mode. Although the concentrations of *PAN*, CH_3ONO_2, and CH_3ONO were known from their determination with the ECD, and thus their contribution to the NO_2 signal of the NO_x detector could be subtracted, still the accuracy in the determination of the NO_2 concentration was low (± 30%) especially when *PAN* and methyl nitrate were high and NO_2 low.

Results and Discussion

Our system was simulated by a 23 reaction mechanism shown in Table 1 using the FACSIMILE software. Although for the sake of completeness the complete set of reactions of OH, HO_2, and other radicals could have been included in the reaction scheme, computer simulations showed that these reactions had no effect on the measured reactants and products and thus they were omitted.

The rate constant used for reaction (1) at 25°C was determined in this work. The corresponding value at 50°C was obtained from the Arrhenius expression of Schurath and Vipprecht [14] multiplied by the ratio of our rate constant at 25°C versus their rate constant at 25°C. The most of the rate constants were obtained from the most recent literature survey available [15]. The rest of the rate constants were obtained from other recent references [16–20]. For those reactions found in their fall off region at 1 atm pressure, the appropriate second order rate constants were calculated using Troe's expression. The literature rate constants were used as reported and no attempt was made to adjust them in order to fit our experimental data.

In addition to the gas phase reactions the heterogeneous removal of *PAN* and peroxy acetyl radicals was also found by computer simulations to be of great

Table 1. Reactions (1)–(22); units $cm^3/mol\ s$ and s^{-1}

Reaction no.	Simulation Mechanism			References
	Reaction	Rate Constants		
		50°C	25°C	
(1)	$PAN \rightarrow CH_3COO_2 + NO_2$	$9.6 \cdot 10^{-3}$	$3.1 \cdot 10^{-4}$	[14], this work
(−1)	$CH_3COO_2 + NO_2 \rightarrow PAN$	$7.0 \cdot 10^{-12}$		[15]
(2)	$2\,CH_3COO_2 \rightarrow 2\,CH_3 + 2\,CO_2 + O_2$	$2.8 \cdot 10^{-12} \cdot 10^{230/T}$		[15]
(3)	$CH_3 + O_2 (+ M) \rightarrow CH_3O_2$	$8.0 \cdot 10^{-13}$	$8.8 \cdot 10^{-13}$	[15]
(4)	$2\,CH_3O_2 \rightarrow 2\,CH_3O + O_2$	$1.2 \cdot 10^{-13}$	$1.4 \cdot 10^{-13}$	[15]
(5)	$2\,CH_3O_2 \rightarrow HCHO + CH_3OH + O_2$	$2.0 \cdot 10^{-13}$		[15]
(6)	$2\,CH_3O_2 \rightarrow CH_3OCH_3 + O_2$	$3.3 \cdot 10^{-14}$	$4.0 \cdot 10^{-14}$	[15]
(7)	$CH_3CO_3 + CH_3O_2 \rightarrow CH_3 + CO_2 + CH_3O + O_2$	$1.8 \cdot 10^{-9} \cdot 10^{-781/T}$		[16]
(8)	$CH_3CO_3 + CH_3O_2 \rightarrow CH_3CO_2H + HCHO + O_2$	$4.1 \cdot 10^{-15} \cdot 10^{912/T}$		[16]
(9)	$CH_3O + O_2 \rightarrow HCHO + HO_2$	$7.2 \cdot 10^{-14} \cdot 10^{-469/T}$		[15]
(10)	$CH_3CO_3 + HO_2 \rightarrow CH_3CO_3H + O_2$	$1.0 \cdot 10^{-13} \cdot 10^{577/T}$		[17]
(11)	$CH_3O + NO_2 \rightarrow CH_3ONO_2$	$1.4 \cdot 10^{-11}$	$1.1 \cdot 10^{-11}$	[15]
(12)	$CH_3O + NO_2 \rightarrow HCHO + HONO$	$1.5 \cdot 10^{-13}$		[18]
(13)	$CH_3 + NO_2 \rightarrow CH_3O + NO$	$2.5 \cdot 10^{-11}$		[19]
(14)	$HO_2 + NO \rightarrow NO_2 + OH$	$3.7 \cdot 10^{-12} \cdot 10^{104/T}$		[15]
(15)	$OH + NO_2 (M) \rightarrow HONO_2$	$1.0 \cdot 10^{-11}$	$1.22 \cdot 10^{-11}$	[15]
(16)	$CH_3O_2 + HO_2 \rightarrow CH_3OOH + O_2$	$1.7 \cdot 10^{-13} \cdot 10^{434/T}$		[15]
(17)	$CH_3O_2 + NO \rightarrow CH_3O + NO_2$	$4.2 \cdot 10^{-12} \cdot 10^{78/T}$		[15]
(18)	$CH_3CO_3 + NO \rightarrow CH_3 + CO_2 + NO_2$	$1.4 \cdot 10^{-11}$		[15]
(19)	$CH_3O + NO \rightarrow CH_3ONO$	$1.9 \cdot 10^{-11}$		[15]
(20)	$CH_3O + NO \rightarrow HCHO + HNO$	$1.3 \cdot 10^{-12}$		[20]
(21)	PAN + wall →	$5 \cdot 10^{-5}$		this work
(22)	CH_3CO_3 + wall →	0.3		[21]

importance. The values we employed for the wall removal of *PAN* and acetyl peroxy radicals in the 4.5 liter flask were $4 \cdot 10^{-5}\,s^{-1}$ and $0.3\,s^{-1}$, respectively. These values are in agreement with the experimentally ones determined in an earlier study [21]: $2 \cdot 10^{-5}\,s^{-1}$ and $0.3\,s^{-1}$ (carried out under the same conditions as in the present work).

PAN−N_2 *System*

The major identified decomposition organo-nitrogen product of the system *PAN* in N_2 was methyl nitrate; it constituted 21 ± 4% of the initial *PAN* concentration, significantly less than the results of Bruckmann and Willner who found methyl nitrate to constitute 60–75% of the initial *PAN* concentration and also of the results of Senum et al. [6] and Wangberg et al. [7] who accounted almost all nitrogen lost from the *PAN* decomposition as methyl nitrate. We believe that the main reason for our low methyl nitrate yield is that a large part of the methoxy radicals react with oxygen present as impurity in N_2 via reaction (9) instead of NO_2 and reaction (11). Most manufacturers state for N_2 5.0 an O_2 impurity of 3 ppmv. Indeed com-

puter simulations showed that in the absence of O_2 the methyl nitrate yield increases to 71% of the initial *PAN* concentration, not different from the value reported by Bruckmann and Willner. The same simulation also showed that NO_2 continued to be a major product accounting for 21% of initial *PAN* concentration. The yield of methyl nitrite, also measured in the reaction products was less than 0.1% of the initial *PAN* concentration. For an initial *PAN* concentration of 440 ppb the calculated N-mass balance based on the yield of methyl nitrate and remaining *PAN* after 200 min reaction time was only 34%. However, we observed an NO_x signal of concentration 210 ppb in addition to *PAN* and methyl nitrate. We can speculate on the nature of the product that is responsible for the additional NO_x signal. From the N-products reported in the literature the excess NO_x signal can be either NO_2 or nitromethane. If this N-product were nitromethane it would have been detected on the ECD; injections of commercially available compound showed that it elutes at known retention time from the column used. Nitromethane was not observed in our experiments nor did we observe another unidentified peak on the ECD. In addition there is kinetic evidence that excludes the formation of nitromethane. The reaction proposed in previous studies [3, 5, 6] to explain the formation of nitromethane is $CH_3 + NO_2 \rightarrow CH_3NO_2$. This reaction is unlikely to occur in our system in the presence of 3 ppm oxygen because of reaction (3). Furthermore, the above reaction is also unlikely to occur in pure *PAN*, because as reported by Yamada et al. [19] it is 10^4 times slower (at 1 Torr) than the bimolecular atom transfer reaction $CH_3 + NO_2 \rightarrow CH_3O + NO$. Therefore we can safely accept that NO_2, which does not respond on the ECD, is formed in the *PAN* thermal decomposition in N_2. The amount of NO_2 formed accounts for 48% of the initial *PAN* concentration and thus raises the N-mass balance to 82%. From the past studies only Bruckmann and Willner observed the formation of NO_2 in the pure *PAN* decomposition, but unfortunately no comparison can be made because they did not report quantitative ratios of both NO_2 and methyl nitrate.

The experimental results with the best computer simulation of the $PAN-N_2$ system is shown in Fig. 1. Two cases were examined in the simulation. First the free radical only mechanism; this case yielded the worst simulation. The second case in addition to the free radical reaction scheme included the heterogeneous removal of *PAN* and acetyl peroxy radicals. The introduction of the wall removal

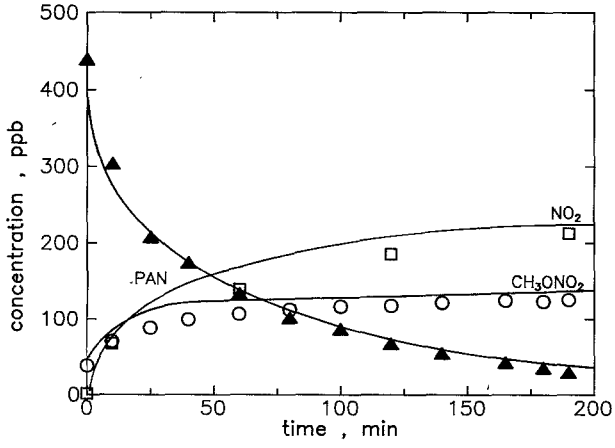

Fig. 1. Time profiles of pure *PAN*, methyl nitrate and NO_2 at 50°C; experimental points: *PAN* ▲, CH_3ONO_2 ○, NO_2 □; Simulation: ———

of acetyl peroxy radical via reaction (22) in the mechanism resulted in a decreased rate of *PAN* destruction and also allowed the formation of NO_2, and thus simulated very well the experimentally determined *PAN*, methyl nitrate, and NO_2 profiles. Kinetic simulations showed that the initial concentration of acetyl peroxy radicals after the introduction of reaction (22) was reduced 2.3 times. A result of this CH_3COO_2 decrease was the reduction of the rates of the very important reaction (2) as well as (7) and (8) and consequently the overall decrease of the *PAN* decay rate and it was more pronounced in the early stages of the reaction. If we included in the simulation scheme the concerted reaction: $PAN \rightarrow CH_3ONO_2 + CO_2$ with the rate constant given by Senum et al. [6] $k = 2.1 \cdot 10^{12} \cdot 10^{-5419/T}$, then the *PAN* profile became too steep, the methyl nitrate increased more above the experimental points whereas the NO_2 remained unaffected.

PAN − O_2 *System*

An argument in favour of the free radical and heterogeneous *PAN* decay and against the Senum et al. homolytic decomposition was the results in the presence of added oxygen. As shown in Fig. 2 the methyl nitrate yield decreased with increasing the O_2 concentration, ending up with zero methyl nitrate formation when $[O_2] > 40\,000$ ppm at 50°C. If there existed a homolytic path to methyl nitrate and carbon dioxide we ought to have always obtained methyl nitrate. In the free radical mechanism however the methoxy radicals, formed mostly from the methyl peroxy radicals, reaction (4), and less from reaction (13) of the methyl radicals with NO_2, are expected on the basis of the free radical mechanism to react either with NO_2: $CH_3O + NO_2 \rightarrow CH_3ONO_2$ (11),
or with O_2: $CH_3O + O_2 \rightarrow HCHO + HO_2$ (9)

The reaction

$$CH_3O + NO_2 \rightarrow HCHO + HONO \quad (12)$$

is 100 times slower than reaction (11) and would not contribute significantly. The

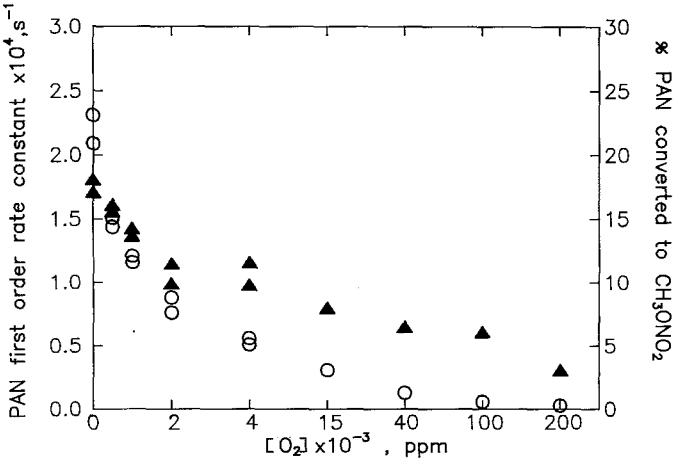

Fig. 2. Effect of added oxygen on the *PAN* decay rate and the methyl nitrate formed; 50°C, initial *PAN* concentration 320–400 ppb; *PAN* ▲, CH_3ONO_2 ○

rate constants favour reaction (11) over reaction (9) by an order of 10^4, but at sufficiently large $[O_2]$ the methyl nitrate yield would decrease to zero.

The decrease of the *PAN* decay rate after the addition of O_2 (also shown in Fig. 2) can also be explained in terms of the free radical only mechanism. Oxygen removes the methoxy radicals via reaction (9) and thus the main route of removal of NO_2 via reaction (11) is limited. Therefore, the NO_2 concentration increases and stabilizes *PAN* via reaction (−1). FACSIMILE simulations showed that indeed the NO_2 concentration increases as the added O_2 increases.

PAN − NO_2 *System*

The purpose of these experiments was to suppress the decay of *PAN* via reaction (−1) with the addition of large amounts of NO_2 and thus allowing the homolytic decay to methyl nitrate and carbon dioxide if this exists. However, as shown in Fig. 3 this was not observed experimentally. The *PAN* decay rate was indeed diminishing up to a minimum at added $[NO_2] = 2.4$ ppm along with the yield of methyl nitrate. Further addition of NO_2 increased the *PAN* decay rate and the methyl nitrate yield. This behaviour was also recently reported by Wangberg et al. [7] who offered no explanation. We believe that the increased *PAN* decay rate is due to NO which we found experimentally to be present in the system at initial concentrations equal to 1.3% of the added NO_2. Although the competition between the stabilizing reaction (−1) and destabilizing reaction (18) is in favour of reaction (−1) mainly because of the small concentration of NO, still at high NO_2 there will be enough NO (compared to *PAN*) to enhance all the reactions of Table 1 involving NO and thus leading to increased *PAN* decay rates. Higher methyl nitrate yields are also expected from the free radical reaction scheme, because at large NO_2 concentrations reaction (11) becomes more significant compared to reaction (9) and thus leads to more methyl nitrate.

This explanation based on the presence of NO was corroborated by the results of FACSIMILE simulations employing the free radical mechanism with the het-

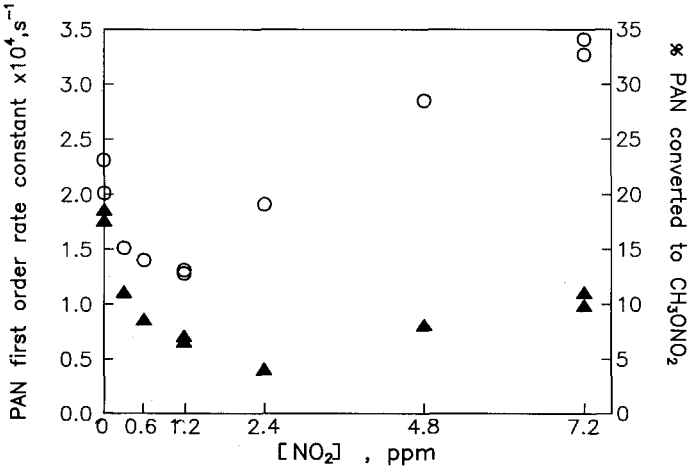

Fig. 3. Effect of added NO_2 on the *PAN* decay rate and on the methyl nitrate formed; 50°C, initial *PAN* concentration 300–400 ppb; *PAN* ▲, CH_3ONO_2 ○

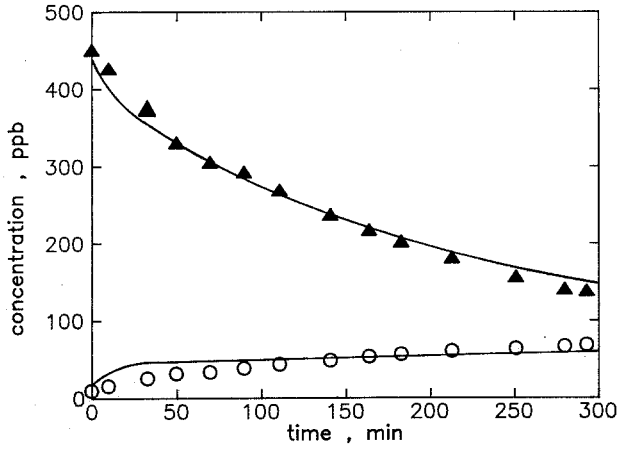

Fig. 4. Time profiles of *PAN* and methyl nitrate in the presence of 1 200 ppb NO_2 at 50°C; experimental points: *PAN* ▲ CH_3ONO_2 ○; simulation: ———

erogeneous contribution (shown in Fig. 4). If NO was not included in the initiating part of the program the resulting simulations (not shown) were very poor. There was no reason to examine the homolytic pathway reported by Senum et al. [6] because the amount of methyl nitrate formed in the simulation was in agreement with the experimentally measured one. It must be pointed out that the O_2 concentration employed in this simulation was 14 ppm. This value can be obtained if we recall that NO_2 was made from an $[O_2]/[NO]$ ratio of 9 : 1. Therefore, introduction of 1 200 ppb NO_2 means the simultaneous introduction of 11 ppm O_2 thus making the total $[O_2] = 14$ ppm.

PAN–NO *System*

The reaction of *PAN* with NO is of great interest because it enhances the *PAN* decay, and also in the presence of large excess NO the measured *PAN* decay rate equals the rate of reaction (1). The first order rate constant for reaction (1) that we obtained at 23.5°C in the 425 l reaction vessel was $3.1 \cdot 10^{-4}\,s^{-1}$ (cf. the plateau

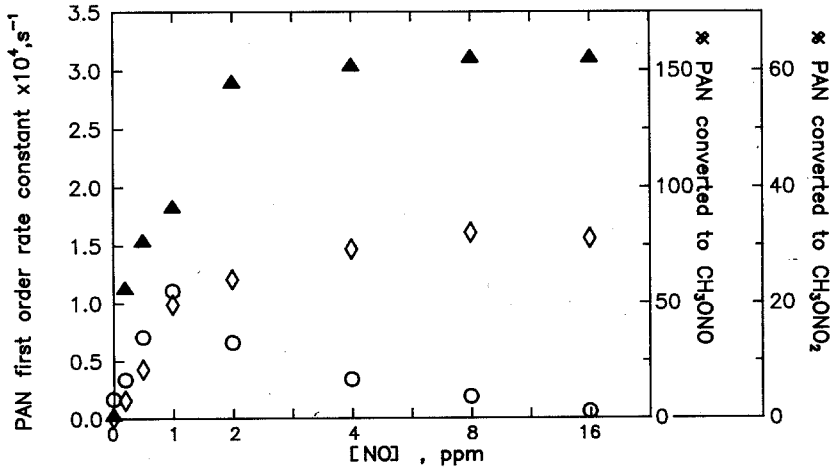

Fig. 5. Effect of added NO on the *PAN* decay rate and on methyl nitrate and methyl nitrite formed; 23.5°C, initial *PAN* concentration 350–400 ppb; *PAN* ▲, CH_3ONO_2 ○, CH_3ONO ◇

region in Fig. 5) whereas in the 4.5 l flask $3.4 \cdot 10^{-4} s^{-1}$. The experimental uncertainty accounts for the 10% difference as indicated from $2\sigma = 0.60$ obtained for the experiments carried out in the small reaction vessel. The value $3.1 \cdot 10^{-4} s^{-1}$ is the same as the value reported by Niki et al. [22] and very close to the value $2.83 \cdot 10^{-4} s^{-1}$ reported by Pate et al. [8] but significantly larger than the corresponding values of $2.2 \cdot 10^{-4} s^{-1}$ and $1.73 \cdot 10^{-4} s^{-1}$ reported by Senum et al. [6] and Wangberg et al. [7], respectively, and approximately 30% lower than the values reported by Schurath and Wipprecht [14], Hendry and Kenly [4], and Cox and Roffey [3].

The major product of these experiments was NO_2. The yield of NO_2 relative to the change of the *PAN* concentration was 1.7 ± 0.3. Simultaneously the $\Delta[NO]/\Delta[PAN]$ observed was 2.7 ± 0.4. One could visualize the formation of one mol of NO_2 to result from reaction (1): $PAN \rightarrow CH_3COO_2 + NO_2$ and one mol from reaction (18): $CH_3COO_2 + NO \rightarrow CH_3CO_2 + NO_2$. Under these conditions one mol of NO would disappear per mol of reacting *PAN*, due to reaction (19), because the obtained yield of methyl nitrite versus *PAN* consumed is close to unity. The remaining almost two mol of consumed NO per mol of reacting *PAN* would be due to reactions (18), (17), and (14).

In contrast to earlier studies [6–8] these experiments showed that the major organo-nitrogen product was methyl nitrite and not methyl nitrate. When a large excess of NO was added the methyl nitrite constituted 75% of the initial *PAN* concentration. Formation of this product, when NO is in large excess, is entirely reasonable to result from reaction (19): $CH_3O + NO \rightarrow CH_3ONO$ and surpass methyl nitrate formed via reaction (11): $CH_3O + NO_2 \rightarrow CH_3ONO_2$. In fact, for added $[NO] > 8$ ppm methyl nitrate was not formed at all. Earlier studies reported methyl nitrite to be a minor product when compared to methyl nitrate [8] whereas others did not observe it at all [6, 7]. The obtained profile of methyl nitrate formed vs. added NO (Fig. 5) shows that its formation depends on the *PAN* and NO concentrations employed and this explains the resuls of Wangberg et al. who reported formation of no methyl nitrate, and also the results of Senum et al. who reported formation of methyl nitrate. Presumably the last mentioned authors did not employ

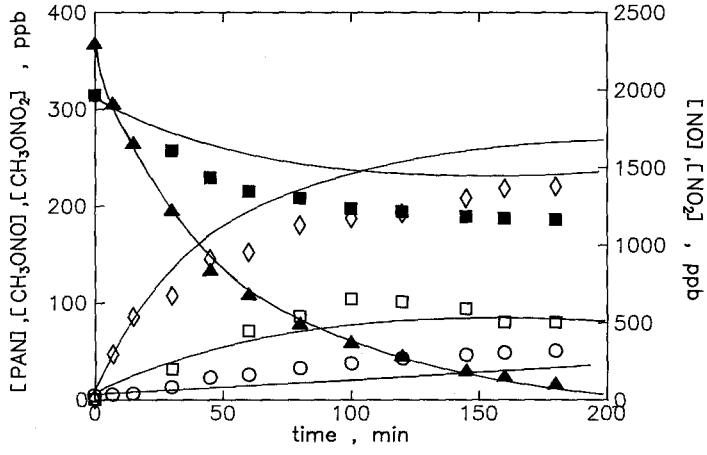

Fig. 6. Time profiles of *PAN* and methyl nitrate in the presence of 2 ppb NO at 23.5°C; experimental points: *PAN* ▲, CH_3ONO_2 ○, CH_3ONO ◇, NO ■, NO_2 □; simulation: ———

a high enough [NO]/[*PAN*] ratio and thus they obtained methyl nitrate. The simulation and experimental results of the system *PAN*+NO in N_2 are shown in Fig. 6. There was no point in testing the contribution of the homolytic pathway, because at 23.5°C the rate constant reported by Senum et al. is only $1 \cdot 10^{-6} s^{-1}$ and would therefore contribute negligible amounts of methyl nitrate. In addition, as seen in Fig. 5, the methyl nitrate formed diminishes towards zero at high NO concentrations. Again the reaction scheme employed in the computer simulations is the one shown in Table 1. *PAN* and methyl nitrate were very well simulated, NO and NO_2 were acceptable in view of their large experimental uncertainties, while methyl nitrite is more than experimentally observed. The ratios of $\Delta[NO_2]/\Delta[PAN]$ and $\Delta[NO]/\Delta[PAN]$ obtained from the simulations were 1.5 and 2.4 respectively, in good agreement with the experimentally determined values.

Acknowledgement

We thank Prof. U. Schurath of the University of Bonn for stimulating discussions and for allowing us to use the FACSIMILE software in their facilities. N. Roumelis also thanks the Hellenic Refineries of Aspropyrgos for a fellowship. This work was financially supported by the Commission of European Communities under contract EV4V-0070-D(B).

References

[1] Singh H. B. (1987) Environ. Sci. Technol. **21**: 320
[2] Stephens E. R. (1969) Adv. Environ. Sci. Technol. **1**: 119
[3] Cox R. A., Roffey M. J. (1977) Environ. Sci. Technol. **111**: 900
[4] Hendry D. G., Kenley R. A. (1977) J. Am. Chem. Soc. **99**: 3198
[5] Bruckmann P. W., Willner H. (1983) Environ. Sci. Technol. **17**: 352
[6] Senum G. I., Fajer R., Gaffney J. S. (1986) J. Phys. Chem. **90**: 152
[7] Wangberg I., Langrova S., Ljungstrom E. (1990) In: Restelli G., Angeletti G. (eds.) Physico-Chemical Behaviour of Atmospheric Pollutants. Klower, Dordrecht, p. 334
[8] Pate C. T., Atkinson R., Pitts J. N. Jr. (1976) J. Environ. Sci. Health-Environ. Sci. Eng. **A11** (1): 19
[9] Nielsen T., Hansen A. M., Thomsen E. L. (1982) Atmos. Environ. **16**: 2447
[10] Gaffney J. S., Fajer R., Senum G. I. (1984) Atmos. Environ. **18**: 215
[11] Blatt A. H. Ed. (1967) Organic Syntheses, Collective Volume 2. Wiley, New York, p. 412
[12] Vogel A. I. (1956) Practical Organic Chemistry, 3rd Ed. Longman, London, p. 306
[13] Roumelis N., Glavas S. (1989) Anal. Chem. **61**: 2731
[14] Schurath U., Wipprecht V. (1979) In: Versino B., Ott H. (eds.) First European Symposium on Physico-Chemical Behaviour of Atmospheric Pollutants, Ispra, Italy, EUR 6621 p. 157
[15] Atkinson R., Baulch D. L., Cox R. A., Hampson R. F. Jr., Kerr J. A., Troe J. (1989) J. Phys. Chem. Ref. Data **18**: 881
[16] Moortgat G., Veyret B., Lesclaux R. (1989) J. Phys. Chem. **93**: 2362
[17] Moortgat G. K., Veyret B., Lesclaux R. (1987) COST 611, WP 2 Meeting. Riso National Laboratory, Denmark, p. 24
[18] Batt L., Rattray G. N. (1979) Int. J. Chem. Kinet. **11**: 1183
[19] Yamada F., Slangle I., Gutman D. (1981) Chem. Phys. Letts. **83**: 409
[20] Atkinson R., Lloyd A. C. (1984) J. Phys. Chem. Ref. Data **13**: 315
[21] Mineshos G., Glavas S., Schurath U. (1990) In: Restelli G., Angeletti G. (eds.) Physico-Chemical Behaviour of Atmospheric Pollutants. Kluwer, Dordrecht, p. 184
[22] Niki H., Maker P. D., Savage C. M., Breitenbach L. P. (1985) Int. J. Chem. Kinet. **17**: 525

Received February 18, 1991. Accepted May 13, 1991